Ground displacements and dilatational strains caused by the 2010-2011 Canterbury earthquakes

J. Beavan
J. Lee
S. Levick
K. Jones

GNS Science Consultancy Report 2012/67
May 2012

GNS SCIENCE
TE PŪ AO

DISCLAIMER

This report has been prepared by the Institute of Geological and Nuclear Sciences Limited (GNS Science) exclusively for and under contract to Tonkin & Taylor Pty Ltd. Unless otherwise agreed in writing by GNS Science, GNS Science accepts no responsibility for any use of, or reliance on any contents of this Report by any person other than Tonkin & Taylor Pty Ltd. and shall not be liable to any person other than Tonkin & Taylor Pty Ltd., on any ground, for any loss, damage or expense arising from such use or reliance.

The data presented in this Report are available to GNS Science for other use from May 2012.

BIBLIOGRAPHIC REFERENCE

Beavan, J.; Levick, S.; Lee, J. and Jones, K. 2012. Ground displacements and dilatational strains caused by the 2010-2011 Canterbury earthquakes, *GNS Science Consultancy Report* 2012/67. 59 p.

CONTENTS

EXECUTIVE SUMMARY ..... **iii**

1.0 INTRODUCTION **1**

2.0 BACKGROUND **2**

2.1 Aerial photography 2
2.2 Sub-pixel correlation 2

3.0 LIDAR COSI-CORR PROCESSING AND RESULTS **3**

3.1 Noise, bias and artefacts 6

4.0 DISLOCATION MODELLING AND RESULTS **8**

5.0 RECOMMENDATIONS **13**

6.0 ACKNOWLEDGMENTS **14**

7.0 REFERENCES **14**

TABLES

Table 1 LiDAR datasets used in the analysis 3
Table 2 Summary of all sets of LiDAR pairs processed 5

FIGURES

Figure 1 Observed (blue) and modelled (red) displacements at GPS sites, and the slip model derived from GPS and DInSAR data for each of the major Canterbury earthquakes. A, 4 September 2010; B, 22 February 2011; C, 13 June 2011; and D, 23 December 2011. Red dots with nearby letters in square brackets (e.g., [a]) are located where the centres of the fault segments would outcrop if extended to the surface. Detailed slip distributions on each fault segment ([a], [b], [c], etc.) are shown in Fig. 2. Some observed GPS displacements have large residuals to the model, particularly for the February 2011 earthquake, and these are downweighted in the inversion. Red and white four-pointed stars show epicentral locations from solution 2012mar11b of S. Bannister (pers. comm., 2012: updated from Bannister et al., 2011). Black square in B shows central Christchurch. 9

Figure 2 Slip magnitude and direction on each of the fault segments modelled as active during the earthquake sequence to date. A-G, I-K, M-O, Labels [a]-[m] correspond to the fault segment labels in Fig. 1. The faults are discretised into 1 $\times$ 1 km patches. Slip vectors showing the motion of the hanging wall relative to the footwall are shown on every other patch. The red-and-white four-pointed stars show hypocentral locations projected on to nearby fault planes. H, L and P, These panels compare the moment tensors from the sum of the fault segments contributing to each earthquake with the GCMT seismological moment tensor solution and the GeoNet regional moment tensor solution. Full moment tensor solutions are shown for the September 2010 and February 2011 earthquakes, and double-couple solutions for the less well constrained June 2011 and December 2011 earthquakes. The velocity scale arrows in panels A, I and M apply to panels A-G, I-K and M-O, respectively. 11

APPENDICES – HARD COPY and CD

Appendix 1 Imagin'Labs Contract Report 1 (of 4) 16
Appendix 2 Imagin'Labs Contract Report 2 (of 4) 21
Appendix 3 Imagin'Labs Contract Report 3 (of 4) 25
Appendix 4 Imagin'Labs Contract Report 4 (of 4) 29
Appendix 5 Summary plots of areal strain and horizontal displacement 33

APPENDICES – CD ONLY

Appendix 6 Ground surface displacements: 04 September 2010 earthquake 55
Appendix 7 Ground surface displacements: 22 February 2011 earthquake 55
Appendix 8 Ground surface displacements: 13 June 2011 earthquake 55
Appendix 9 Ground surface displacements: 23 December 2011 earthquakes 55

EXECUTIVE SUMMARY

Aircraft-based LiDAR (Light Detection And Ranging) data have been collected on behalf of various agencies over Christchurch and surrounding regions both before and after the four main earthquakes that have occurred to date in the ongoing Canterbury earthquake sequence.

Tonkin & Taylor Pty Ltd (T&T), working on behalf of the New Zealand Earthquake Commission (EQC), contracted GNS Science (GNS) to use pairs of these data (e.g., one before and one after a particular earthquake) to determine horizontal ground displacements and dilatational (or areal) ground strains caused by the earthquakes, using a technique known as sub-pixel correlation. GNS in turn subcontracted part of this work to Imagin'Labs of Pasadena, California, whose staff are expert in sub-pixel correlation using the COSI-Corr software package (Leprince et al., 2007).

Using the LiDAR data available, the technique has typically enabled ground displacements due to lateral spreading and other ground failure mechanisms to be reliably detected when the displacements are larger than a few tens of centimetres. This detectability level varies between images and between different parts of the same image, depending on various noise sources.

As well as displacements due to localised ground failure, the Christchurch region experienced tectonic ground displacements due to the elastic response of the Earth to the slip between the two sides of the faults that generated the earthquakes. As a second part of the project, T&T contracted GNS to estimate these tectonic ground displacements for each of the major earthquakes. This was achieved using a technique known as dislocation modelling. The data contributing to the modelling were (1) ground displacements measured at individual survey marks using the Global Positioning System (GPS) by GNS and Land Information New Zealand (LINZ), and (2) satellite radar images available from a variety of international space agencies.

This report details the background to the project, discusses the data preparation and processing, and makes recommendations for future usage of LiDAR data to determine horizontal ground displacements and strain using sub-pixel correlation.

A particular recommendation is that the LiDAR dataset needed for correlation processing is the full point cloud dataset. Therefore, correlation processing to determine horizontal displacements can be initiated as soon as the second of a pair of LiDAR data has been acquired and georeferenced. There is no need to wait for the LiDAR returns to be classified.

1.0 INTRODUCTION

Using airborne LiDAR data collected before and after the four main earthquakes to date in the ongoing Canterbury seismic sequence (Mw 7.1, 4 September 2010, Darfield; Mw 6.2-6.3, 21 February 2011, Christchurch; Mw 6.0, 13 June 2011, Christchurch; two large earthquakes totalling Mw 6.0, 23 December 2011, Christchurch) we have constructed horizontal ground displacements and dilatational (or areal) strains caused by each of the earthquakes separately, and for combinations of the various earthquakes. This was done by comparing pairs of LiDAR surface elevation models collected before and after each earthquake using a "sub-pixel correlation" technique.

The project results were for the use of Tonkin & Taylor Pty Ltd (T&T), on behalf of the Earthquake Commission (EQC) and later also the Canterbury Earthquake Recovery Authority (CERA), to provide information on land damage due to the earthquakes (such as lateral spreading and liquefaction), and to contribute to subsequent classification of the land into "red-zone" (not to be rebuilt), "green-zone" (OK to rebuild) and intermediate zones.

A second part of the project involved providing T&T with predicted 3-D tectonic ground displacements (i.e., displacements resulting directly from the earthquake faulting, excluding the land damage). These were generated by "dislocation modelling" to infer the locations of the causative faults and the slip between the two sides of the faults using GPS data collected on the ground by various agencies, together with synthetic aperture radar data collected by the radar satellites of a number of international space agencies. The dislocation models were then used to predict the displacements over the whole Christchurch region. T&T used these displacements to separate the tectonic displacements from the displacements measured in the LiDAR correlation processing, in order to isolate the displacements due to land damage.

The main processing of the LiDAR images has been done under contract by Dr Sébastien Leprince of Imagin'Labs Corporation, Pasadena, California using the largely-automated COSI-Corr image registration and sub-pixel correlation software developed at California Institute of Technology by Leprince and others (2007).

GNS Science (GNS) prepared the LiDAR full point cloud data as 1 m surface elevation grids for processing, reviewed the results, interacted closely with Imagin'Labs to provide data products most suited to T&T's requirements, and facilitated the interface between Imagin'Labs and T&T. The 1 m grid was chosen because there were typically 1-2 laser strikes per square metre in the LiDAR datasets.

The primary results were provided from Imagin'Labs in ENVI format, and were formatted by GNS for T&T in GeoTiff and ESRI shapefile format, and as Google Earth overlays. These files give displacement vectors on an 8-m grid for LiDAR pairs involving the lower-quality 2003 LiDAR dataset, and a 4-m grid for all other LiDAR pairs. Also provided in the same format are smoothed areal strain estimates, typically over a 3x3 or 5x5 pixel region, leading to 12-20 m spatial resolution for most LiDAR pairs, or about 40 m for pairs involving the 2003 LiDAR. It is these files that are used by T&T as a component of their detailed land-damage assessments, including the presentation of the results on scalable Google Earth overlays.

The results are also provided as lower resolution pdf maps showing horizontal displacements on a 56 m grid overlaid on the smoothed areal strains. These are reproduced in this report and are intended for a quick appreciation of the results.

2.0 BACKGROUND

2.1 Aerial photography

Following the September 2010 Darfield earthquake, Japanese scientists Professors Masanori Hamada, Ömer Aydan and Iwao Yasuda visited Canterbury and worked with GNS and University of Canterbury engineers to assess land damage, including lateral spreading and liquefaction, in Christchurch and Kaiapoi. They obtained medium-resolution aerial photographs from before and after the earthquake, the acquisition of the latter having been coordinated by the Ministry of Civil Defence and Emergency Management (MCDEM), and processed these back in Japan using an image registration technique originally published by Hamada et al. (1986). They analysed some relatively small regions at Dallington near the Avon River and in Kaiapoi that showed metre-level lateral-spreading displacements. The images were sent back to New Zealand but not distributed widely; they have now been published in Aydan et al. (2012).

T&T and others were very interested in these images as they provided precisely the sort of data they needed to help with land-damage assessments, both in verifying displacements recorded on the ground and in interpolating between areas where ground measurements had not been made or were impractical. This interest was magnified following the 22 February 2011 earthquake.

GNS explored various options for having our Japanese colleagues do more image registration work for both the September 2010 and February 2011 earthquakes, but over a much wider region than their initial study. These options included sending a GNS staff member to Japan to learn the software. This was difficult because all suitable GNS staff were fully engaged on other work, and was made even more uncertain following the Mw 9.1 Tohuku-oki earthquake in March 2011. GNS was also under the impression that Hamada's method required considerable manual intervention that would not provide the early results requested by T&T over a wide region, particularly with the lead-in time required to learn the software and import it back to GNS.

2.2 Sub-pixel correlation

GNS staff were also aware of a largely automated sub-pixel image registration software package ("COSI-Corr") that had been developed at California Institute of Technology (Leprince et al., 2007) and since used widely. We experimented with a publicly-released version of the software using SPOT-4 and WorldView-1 images supplied by the USGS through the International Disaster Charter. The technique showed promise but the publicly available version of COSI-Corr did not allow processing of WorldView-2 images or LiDAR data.

On 27 April 2011, Shaun Levick and John Beavan attended a meeting called by Sjoerd van Ballegooy at T&T in Christchurch, and including representatives from a number of other interested agencies. At that meeting, Sjoerd impressed on us the urgent need for horizontal ground displacement results from some form of remote sensing.

We considered that the relatively highly-automated COSI-Corr processing would provide results more quickly and over a wider area than the Japanese methodology.

3.0 LIDAR COSI-CORR PROCESSING AND RESULTS

Later on 27 April we asked Dr Leprince if he would be available to assist us in the processing. It was an opportune time as he was in the process of setting up a spin-off company to do precisely this kind of work and our contract would be a welcome boost to getting the company off the ground. We considered the possibility of sending a staff member to California to learn the software at first-hand, but this again had problems with GNS staff availability, as well as possible delays in purchasing necessary hardware at GNS and issues with licensing of parts of the software that were not publicly released. In the ensuing discussions we also realised that the LiDAR data already collected under various funding sources was probably suitable for COSI-Corr processing.

We sent a test set of the LiDAR data to Imagin'Labs Corporation (the name of the company when it was formally registered in June 2011), consisting of 1 metre gridded versions of the 2010 post-September and 2011a post-February full point cloud LiDAR datasets. Imagin'Labs tried a number of approaches to the data processing and presentation of results, with a large amount of telephone and e-mail feedback between GNS and Imagin'Labs, between GNS and T&T, and occasional e-mails involving all three parties.

During these tests we developed in broad outline the deliverables described in Section 1.0 above. While the areal strain estimates are a robust product of the COSI-Corr analysis, Imagin'Labs initially advised us against placing too much trust in the horizontal ground displacement vector results. Instead, they recommended using a "profile tool" in the COSI-Corr software that would draw relative displacements along selected profiles. However, when it was reported by T&T that the vector results were giving excellent agreement with field measurements where they had been made, and because the processing could be much more automated, we settled on deriving the horizontal vectors on a grid.

The LiDAR data sets used in the analysis are shown in Table 1 and are discussed further below.

Table 1 LiDAR datasets used in the analysis

GNS label	Acquisition dates	Earthquake	Contractor	Client
2003	6-9 Jul 2003	Before Sep 2010	AAM	CCC
2005	21-24 Jul 2005	Before Sep 2010	AAM	WDC
2010_north	5 Sep 2010	After Sep 2010	NZAM	MCDEM
2010_central	5 Sep 2010	After Sep 2010	NZAM	MCDEM
2010_west	5 Sep 2010	After Sep 2010	NZAM	MCDEM
2011a	8-10 Mar 2011	After Feb 2011	NZAM	MCDEM
2011b	20-30 May 2011	After Feb 2011	AAM	CCC
2011c	18 Jul - 3 Sep 2011	After Jun 2011	NZAM	EQC
2012a	17-18 Feb 2012	After Dec 2011	NZAM	EQC

AAM = Australian Aerial Mapping Ltd; NZAM = New Zealand Aerial Mapping Ltd; CCC = Canterbury City Council; WDC = Waimakariri District Council; EQC = Earthquake Commission; MCDEM = Ministry of Civil Defence and Emergency Management on behalf of NZ Government.

The 2010 LiDAR dataset unfortunately only covered a limited area of Christchurch and Kaiapoi, in the regions most badly affected by the September 2010 quake. The 2010-2011a pair therefore did not give a full picture of the February displacements, especially in the Port Hills and the region just to their north. In addition, the three sub-regions (central, northern and western) of the 2010 LiDAR were flown in different flight directions, which meant that the data had to be processed as three separate pairs for best results.

Following the success of the test, GNS contracted Imagin'Labs to do further work involving the 2003, 2010 and 2011a LiDAR. It later transpired that LiDAR had been flown over Kaiapoi in 2005, and this was added to the contract as a pre-September 2010 view of the Kaiapoi region. (LiDAR flown by Selwyn District Council in 2008 was not included in the COSI-Corr analysis as the region was considered to have experienced little ground damage with high economic impact.)

In the case of the 2003-2010 pair, the specifications (e.g., capture density) and older instrumentation used for the 2003 data were of sufficiently low quality that there was no gain in analysing the 2003-2010 pair in three separate sub-regions[1].

While this processing was going on, a further post-February 2011 LiDAR survey was being organised, because the March 2011 survey did not provide complete coverage over the area where lateral motion was visible on the ground. This 2011b survey was flown from 20-30 May, and was followed soon after by the 13 June 2011 earthquake. This necessitated a further post-June LiDAR survey (2011c) that did not get flown for some time due to snow cover and weather considerations. Most of the possible LiDAR pairs from these surveys were processed by Imagin'Labs, under two additional contracts.

Following the 23 December 2011 earthquakes a further LiDAR dataset was acquired and a subset of the possible LiDAR pairs from this and earlier surveys were processed by Imagin'Labs, under an additional (fourth) contract.

As well as the surveys that crossed the times of earthquakes, we took the opportunity to process the 2011a-2011b pair in order to evaluate the noise level in the method during a time when only moderate aftershocks occurred. This showed ground displacement noise of 10-15 cm in many areas of the image, despite a number of problems in the 2011a dataset (Appendix 2). This suggests that 2-D displacements larger than ~40 cm, and probably lower for the best datasets (e.g., 2011b - 2011c), should be reliably detected over large parts of each image pair (excluding regions where severe noise problems were encountered). It is not part of this contract to do a detailed study of noise levels in the horizontal displacement measurements, nor of noise levels in the areal strain estimates.

[1] Considerable effort was expended by AAM to reprocess the 2003 dataset so that the geoid model was compatible with that used for the later surveys. This is important for assessing the bare-earth elevation (DEM) difference between 2003 and later, post-earthquake, datasets. But it is not important for the COSI-Corr processing, as a small slope has an insignificant effect on the horizontal pixel offsets measured by COSI-Corr. For a slope of 1 m over a 5 km distance, the horizontal error is about 0.02%.

Details of the processing, results, and problems encountered are described in Appendices 1-4, in reports prepared by Imagin'Labs. It is important to read these reports to understand some of the limitations of the method and the problems encountered with some of the image pairs.

Some of the earthquake-crossing pairs included overlapping data for the same earthquake(s) (e.g., 2011a-2011c and 2011b-2011c; see Table 2). In one of these cases T&T requested GNS to provide data from pairs involving 2011b data in preference to 2011a data, because the 2011b data had been proved to be of better quality than 2011a in the COSI-Corr analysis (Appendix 2). In the other case, we were requested to use data closest to the earthquake; specifically to use the 2005 data for Kaiapoi rather than the 2003 data. Instructions on how to combine the individual images into nine maps, each spanning one, two, three or all four earthquakes, are provided in Table 2.

The summary areal strain and displacement maps are printed in Appendix 5, Figures A1-A21, and are also included on the CD accompanying this report. The pdf files on the CD are at high resolution and can be expanded to view small areas of the images in detail.

Table 2 Summary of all sets of LiDAR pairs processed

LiDAR pair	Ref. in Appendix 5	Notes on combining images
September 2010 earthquake		
2003 - 2010	Figure A1	Master image
2005 - 2010	Figure A2	Join with 2003-2010; no overlap
February 2011 earthquake		
2010_central - 2011a	Figure A3	Superceded by 2010_central-2011b; not needed
2010_northern - 2011a	Figure A4	Combine the part north of the Waimakariri River with 2010-2011b_northern; discard the southern part of the image
2010_central - 2011b	Figure A5	Master image
2010_northern - 2011b	Figure A6	Join the combined 2010-2011a_northern/2010-2011b_northern with 2010_central-2011b; no overlap
2010_western - 2011b	Figure A7	Join with 2010_central-2011b; no overlap
June 2011 earthquake		
2011a - 2011c	Figure A8	Combine the region north of the Waimakariri River with 2011b-2011c; discard the southern part of the image
2011b - 2011c	Figure A9	Master image
December 2011 earthquake		
2011c – 2012a	Figure A10	Master image

LiDAR pair	Ref. in Appendix 5	Notes on combining images
September 2010 + February 2011 earthquakes		
2003 - 2011a	Figure A11	Superceded by 2003-2011b; not needed
2005 - 2011a	Figure A12	Join with 2003-2011b; no overlap
2003 - 2011b	Figure A13	Master image
February 2011 + June 2011 earthquakes		
2010_central - 2011c	Figure A14	Master image
2010_northern - 2011c	Figure A15	Join with 2010_central-2011c; no overlap
2010_western - 2011c	Figure A16	Join with 2010_central-2011c; no overlap
June 2011 + December 2011 earthquakes		
2011b – 2012a	Figure A17	Master image
September 2010 + February 2011 + June 2011 earthquakes		
2003 - 2011c	Figure A18	Master image
2005 - 2011c	Figure A19	Join with 2003-2011c; no overlap
September 2010 + February 2011 + June 2011 + December 2011 earthquakes		
2003 – 2012a	Figure A20	Master image
Noise study		
2011a - 2011b	Figure A21	Master image

3.1 Noise, bias and artefacts

We briefly discuss the origins of noise, bias and artefacts in the sub-pixel correlation images. This sub-section was mostly provided by Sébastien Leprince.

Noise. Noise in the horizontal displacements measured, hence also in the areal strain, is due to three main sources: (1) temporal changes (e.g., change in vegetation cover, which is very evident between the March (2011a) and May (2011b) data, for instance inside the horseshoe area); (2) lack of features for correlation, which is very evident in flat areas such as agricultural fields; and (3) limited resolution of the gridded data (in practice, when correlation doesn't fail, it's accurate to about 1/10 of the pixel size over small patches).

Bias in horizontal displacement. Most bias is due to: (1) LiDAR pointing inaccuracies; and (2) flat surfaces with no features, which often will record zero displacement. As for the noise, not much can be done when not enough features to correlate on are present. However, LiDAR pointing inaccuracies cannot be neglected in the data studied. In most data sets, pointing inaccuracies produced jitter artefacts in the displacement field. The jitter artefacts, mostly sinusoidal in both across-track and along-track direction of the flight path, had an

average amplitude on the order of 30 cm, sometimes peaking at more than 50 cm. This bias makes it challenging to deliver displacement measurement with less than 10 cm of noise. Although Imagin'Labs were able to remove most of the bias during this work, such post-processing was not possible in some instances, in particular in areas of large noise due to temporal decorrelation. Such bias removal is also data dependent and often requires tedious manual adjustment, slowing the response time of the product delivery in operational situations.

Jitter artefacts. These are generally caused by: (1) inaccurate intertial measurement unit (IMU) attitude angles (roll, pitch, yaw); (2) insufficient time sampling of the IMU; (3) inaccurate or miscalibration of the LiDAR boresight angles; (4) baseline between IMU and LiDAR sensor; and (5) clock synchronisation problems between GPS and IMU, etc. In designing the LiDAR survey, these sources of uncertainty should be discussed with the company providing the survey.

Flight paths. From Imagin'Labs experience, it is assumed some bias will always be present at some scale. Most biases are correlated with the flight path (along-track and across-track). To make potential biases easy to remove, it is usually best to have parallel flight paths between all the surveys. This is because biases then end up being in only one direction. When flight paths cross, this generates crossing bias patterns, which are challenging to remove. Imagin'Labs noticed crossing bias patterns in almost all pairs processed in this work.

4.0 DISLOCATION MODELLING AND RESULTS

Models of the slip distributions and fault locations for each earthquake were calculated by established dislocation modelling methods using GPS data and synthetic aperture radar data collected before and after each earthquake. The data processing and modelling is described in a series of papers (Beavan et al., 2010, 2011, 2012) so we do not go into detail here about the methodology and results. The locations of the modelled faults are shown in Figure 1, and the inferred slip distributions between the two sides of each fault surface are shown in Figure 2.

The models were used to predict the 3-D ground displacements on a grid of points at nominally 250 m spacing covering the region of the LiDAR surveys. These have been supplied to T&T as Excel spreadsheets. The latest versions of these spreadsheets are included on the CD accompanying this report as Appendices 6-9. Some of the spreadsheets have been updated since draft versions were supplied to T&T in 2011 and early 2012. However, any changes are small enough that they should have no impact on uses to which the draft spreadsheets have already been put by T&T.

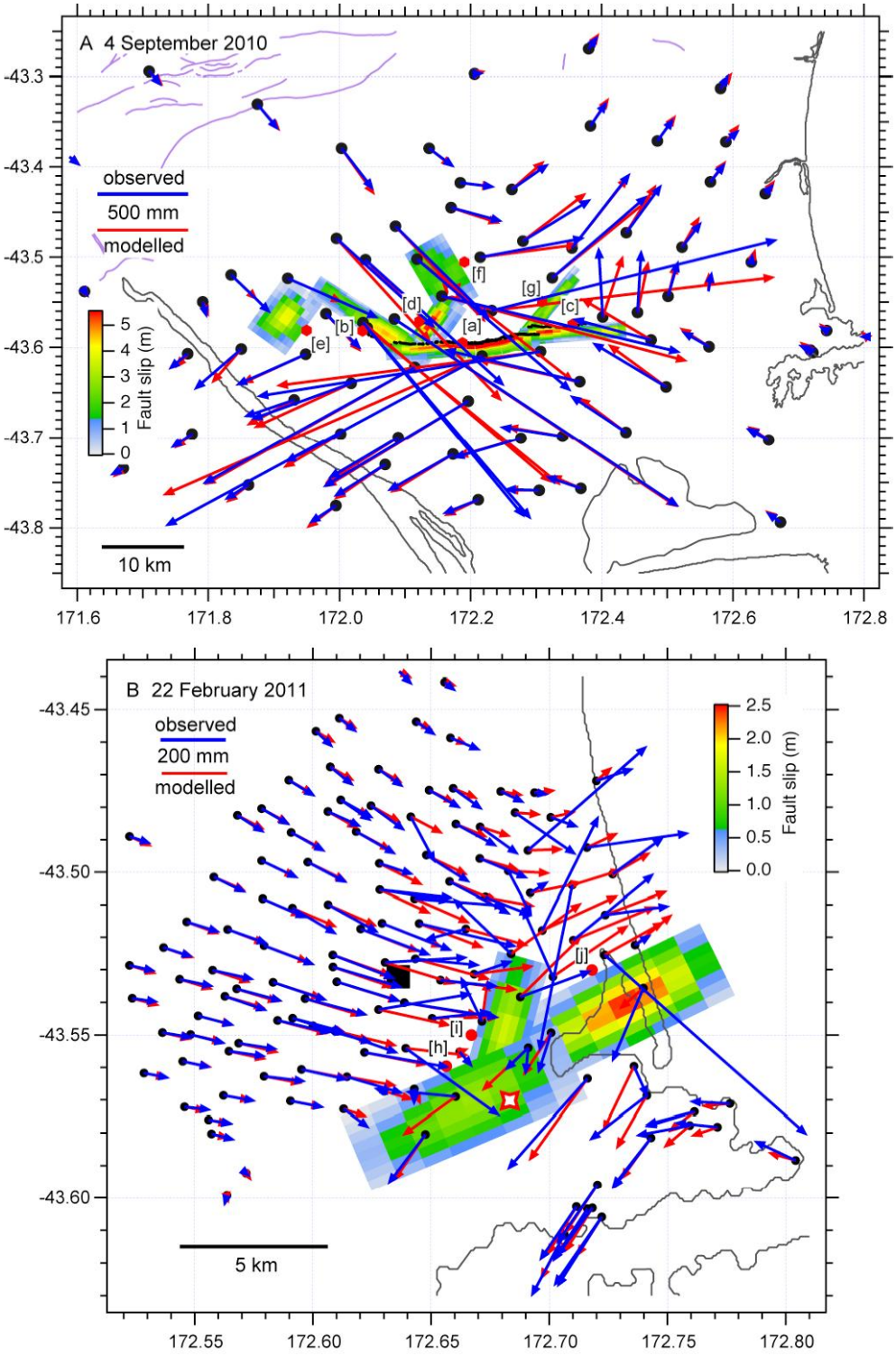

Figure 1 Observed (blue) and modelled (red) displacements at GPS sites, and the slip model derived from GPS and DInSAR data for each of the major Canterbury earthquakes. A, 4 September 2010; B, 22 February 2011; C, 13 June 2011; and D, 23 December 2011. Red dots with nearby letters in square brackets (e.g., [a]) are located where the centres of the fault segments would outcrop if extended to the surface. Detailed slip distributions on each fault segment ([a], [b], [c], etc.) are shown in Fig. 2. Some observed GPS displacements have large residuals to the model, particularly for the February 2011 earthquake, and these are downweighted in the inversion. Red and white four-pointed stars show epicentral locations from solution 2012mar11b of S. Bannister (pers. comm., 2012: updated from Bannister et al., 2011). Black square in B shows central Christchurch.

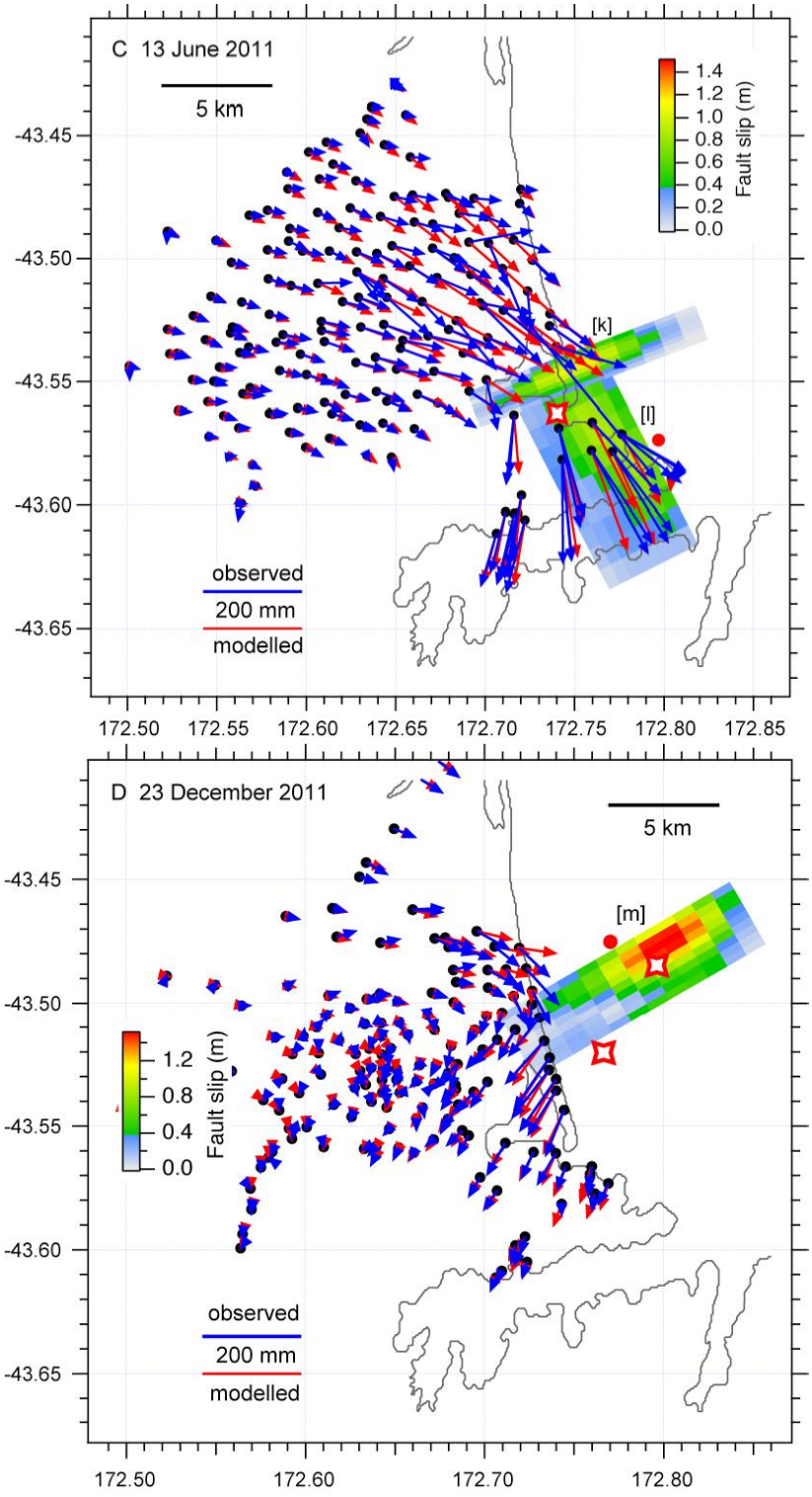

Figure 1 See caption on previous page.

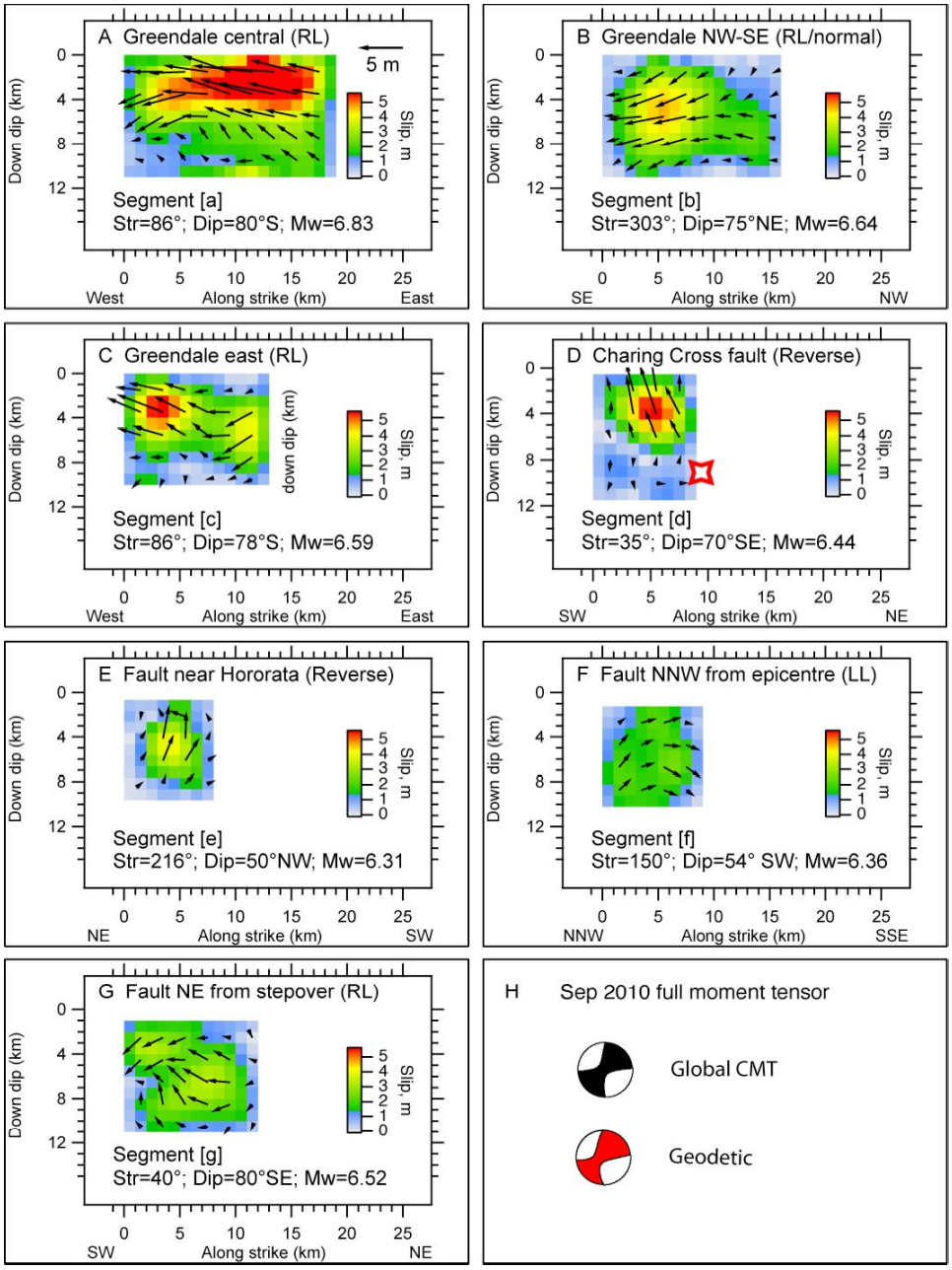

Figure 2 Slip magnitude and direction on each of the fault segments modelled as active during the earthquake sequence to date. A-G, I-K, M-O, Labels [a]-[m] correspond to the fault segment labels in Fig. 1. The faults are discretised into 1 × 1 km patches. Slip vectors showing the motion of the hanging wall relative to the footwall are shown on every other patch. The red-and-white four-pointed stars show hypocentral locations projected on to nearby fault planes. H, L and P, These panels compare the moment tensors from the sum of the fault segments contributing to each earthquake with the GCMT seismological moment tensor solution and the GeoNet regional moment tensor solution. Full moment tensor solutions are shown for the September 2010 and February 2011 earthquakes, and double-couple solutions for the less well constrained June 2011 and December 2011 earthquakes. The velocity scale arrows in panels A, I and M apply to panels A-G, I-K and M-O, respectively.

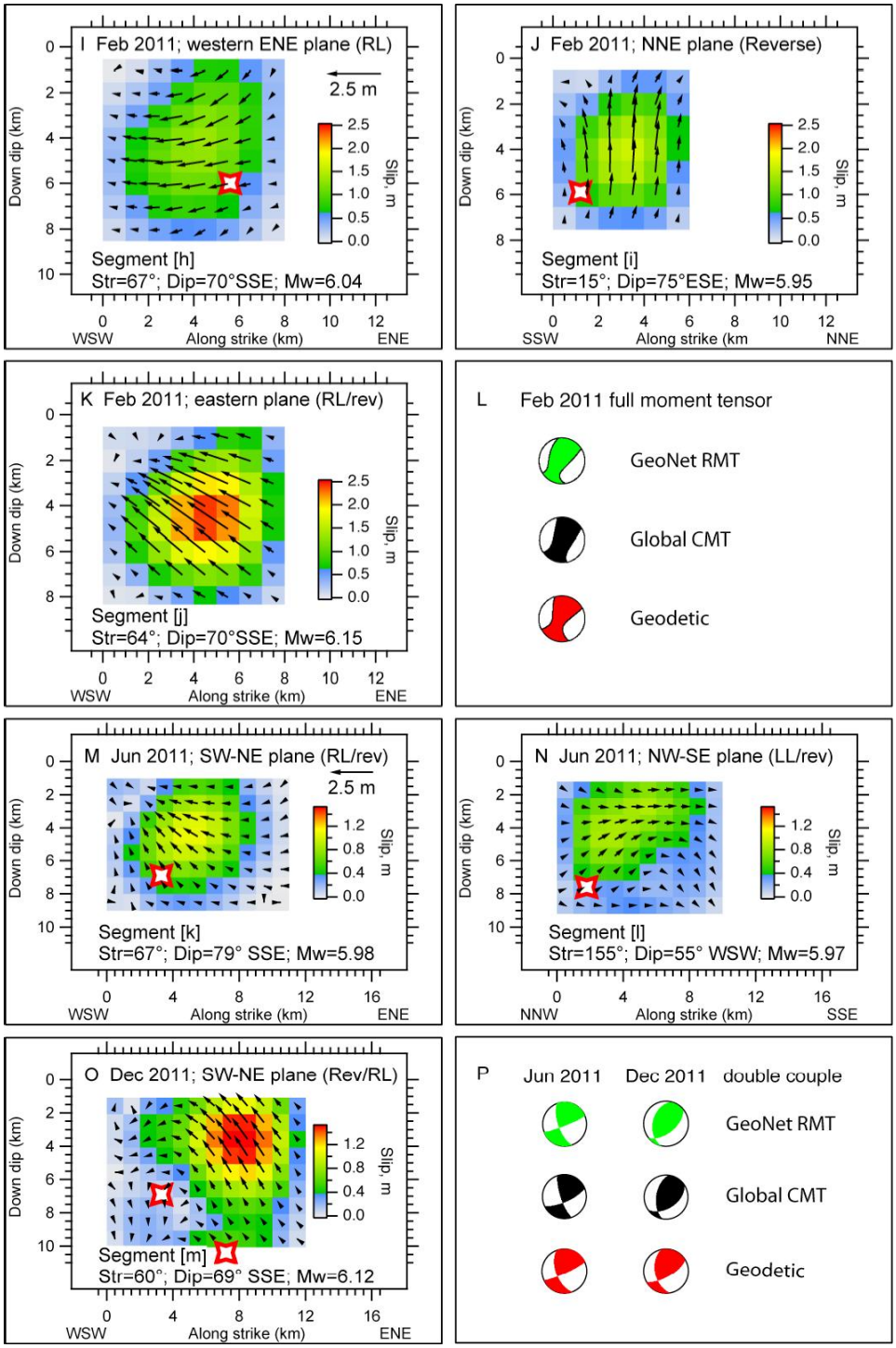

Figure 2 See caption on previous page.

5.0 RECOMMENDATIONS

The following recommendations regarding the collection of LiDAR data are aimed at obtaining high quality sub-pixel correlation measurements of horizontal ground displacements from LiDAR data. We believe they will prove useful in the event of a future natural disaster event in Christchurch or elsewhere. The recommendations do not apply only to LiDAR acquired following such an event, but also to all acquisitions that might potentially be useful as a pre-event dataset.

1. The LiDAR dataset needed for correlation processing is the full point cloud dataset. Therefore, correlation processing to determine horizontal displacements can be initiated as soon as the second of a pair of LiDAR data has been acquired and georeferenced. There is no need to wait for the LiDAR returns to be classified.

2. The LiDAR acquisition plan should aim for at least 2 strikes per square metre, and preferably as many as 4-5. (In other work similar to this, Imagin'Labs has obtained very good results with data gridded at 40-50 cm.) Increasing the strike density by lowering the flight altitude would also decrease jitter that is due to uncertainty on the roll, pitch and yaw angles recorded by the IMU (but would require increased flight time and therefore cost).

3. The LiDAR survey should be designed to minimise jitter artefacts, as discussed at the end of Section 3.1 above.

4. It is important to aim for consistency in flight line orientation between and within surveys if conditions allow, so that these effects are consistent and easier to remove in post-processing.

5. For this type of work it is worth waiting for good flying conditions to minimize aircraft jitter, though this would not always be feasible in a disaster situation.

6. A more regular collection of LiDAR survey data would make sub-pixel correlation work easier in the event of a disaster. Correlation between the 2003/05 and 2010-2011 surveys proved to be quite challenging. (However, we recognise that this is probably not financially feasible.)

7. The recommendations above should be applied as far as possible to all LiDAR datasets acquired in New Zealand, as one never knows when such a dataset will become important as a pre-disaster dataset.

8. One or more people from GNS should become familiar with the public version of COSI-Corr software, and become proficient in processing SPOT and WorldView imagery. Although Imagin'Labs now offers a commercial service for advanced processing, we believe that GNS staff will be better able to interact with Imagin'Labs if they are comfortable with the technique and products.

6.0 ACKNOWLEDGMENTS

We thank the New Zealand Government (MCDEM) for arranging access to the LiDAR data collected by NZAM and AAM, and also Christchurch City Council and the Earthquake Commission for permission to use the LiDAR data. We thank Land Information New Zealand for supplying some of the GPS data, particularly for the February and June earthquakes, and the Japanese, European, Italian and German space agencies for acquiring and supplying synthetic aperture radar data from the ALOS/PALSAR, Envisat, Cosmo-SkyMed and TerraSAR-X satellites, respectively. We are particularly grateful for the radar data that were provided free-of-charge. We thank Sébastien Leprince of Imagin'Labs for giving priority to the Christchurch COSI-Corr processing, and Sébastien, Sjoerd van Ballegooy, Bruce Deam, and Dick Beetham for discussions. We thank Dick Beetham and Salman Ashraf for their reviews of this report, and Peter Wood for his careful and detailed review of an earlier draft.

7.0 REFERENCES

Aydan, O., M. Hamada, D. Beetham, and I. Yasuda (2012). Evaluation of ground liquefaction and lateral spreading caused by the 2010 and 2011 Canterbury earthquakes, International Conf. on Earthquake Geotech. Eng., From Case History to Practice, 23-25 Jan 2012, Aswan, Egypt.

Bannister S., B. Fry, M. Reyners, J. Ristau, and H. Zhang (2011). Fine scale relocation of aftershocks of the 22 February M_W 6.2 Christchurch earthquake using double difference tomography. Seismol. Res. Lett., 82(6): 839-845. doi: 10.1785/gssrl.82.6.839

Beavan, J., S. Samsonov, M. Motagh, L. Wallace, S. Ellis, and N. Palmer (2010). The Darfield (Canterbury) earthquake: geodetic observations and preliminary source model. Bulletin New Zealand Society for Earthquake Engineering, 43(4): 228-235. (Available at: http://www.gns.cri.nz/Home/News-and-Events/Media-Releases/Most-damaging-quake-since-1931/Canterbury-quake/Satellite-radar-results; accessed 24 Feb 2012)

Beavan, J., E. Fielding, M. Motagh, S. Samsonov, and N. Donnelly (2011). Fault location and slip distribution of the 22 February 2011 Mw 6.2 Christchurch, New Zealand, earthquake from geodetic data. Seismol. Res. Lett., 82(6): 789-799. doi: 10.1785/gssrl.82.6.789

Beavan, J., M. Motagh, E. Fielding, N. Donnelly, and D. Collett (2012). Fault slip models of the 2010-2011 Canterbury, New Zealand, earthquakes from geodetic data, and observations of post-seismic ground deformation, N. Z. J. Geol. Geophys., in review.

Hamada, M., S. Yasuda, R. Isoyama, and K. Emoto (1986). Study on liquefaction-induced permanent ground displacements, Assoc. for the Development of Earthquake Prediction in Japan, 1, 87 pp.

Leprince, S., S. Barbot, F. Ayoub, and J.-P. Avouac (2007). Automatic and precise orthorectification, coregistration, and subpixel correlation of satellite images, application to ground deformation measurements, IEEE Trans. on Geoscience and Remote Sensing, 45(6), 1529-1558.

APPENDICES

APPENDIX 1 IMAGIN'LABS CONTRACT REPORT 1 (OF 4)

This appendix (4 pages in total) is also supplied as a .pdf file on the accompanying CD.

APPENDIX 2 IMAGIN'LABS CONTRACT REPORT 2 (OF 4)

This appendix (3 pages in total) is also supplied as a .pdf file on the accompanying CD.

APPENDIX 3 IMAGIN'LABS CONTRACT REPORT 3 (OF 4)

This appendix (3 pages in total) is also supplied as a .pdf file on the accompanying CD.

APPENDIX 4 IMAGIN'LABS CONTRACT REPORT 4 (OF 4)

This appendix (3 pages in total) is also supplied as a .pdf file on the accompanying CD.

APPENDIX 5 SUMMARY PLOTS OF AREAL STRAIN AND HORIZONTAL DISPLACEMENT

This appendix consists of figures (21 pages in total) that are also supplied as high resolution .pdf files on the accompanying CD.

The file names on the CD include the figure number (e.g., “FigA6”).

Each plot is labelled with the LiDAR pair.

A cross reference between the figure numbers and the LiDAR pairs is included in Table 2 of the main text.

APPENDIX 6 GROUND SURFACE DISPLACEMENTS: 04 SEPTEMBER 2010 EARTHQUAKE

This appendix consists of an Excel spreadsheet located on the accompanying CD. The spreadsheet contains the tabulated values of horizontal and vertical tectonic ground displacement predicted by the dislocation model of the 4 September 2010 earthquake.

The displacements are calculated on a nominally 250-metre grid covering the region of the LiDAR surveys.

APPENDIX 7 GROUND SURFACE DISPLACEMENTS: 22 FEBRUARY 2011 EARTHQUAKE

This appendix consists of an Excel spreadsheet located on the accompanying CD. The spreadsheet contains the tabulated values of horizontal and vertical tectonic ground displacement predicted by the dislocation model of the 22 February 2011 earthquake.

The displacements are calculated on a nominally 250-metre grid covering the region of the LiDAR surveys.

APPENDIX 8 GROUND SURFACE DISPLACEMENTS: 13 JUNE 2011 EARTHQUAKE

This appendix consists of an Excel spreadsheet located on the accompanying CD. The spreadsheet contains the tabulated values of horizontal and vertical tectonic ground displacement predicted by the dislocation model of the 13 June 2011 earthquake.

The displacements are calculated on a nominally 250-metre grid covering the region of the LiDAR surveys.

APPENDIX 9 GROUND SURFACE DISPLACEMENTS: 23 DECEMBER 2011 EARTHQUAKES

This appendix consists of an Excel spreadsheet located on the accompanying CD. The spreadsheet contains the tabulated values of horizontal and vertical tectonic ground displacement predicted by the dislocation model of the 23 December 2011 earthquakes.

The displacements are calculated on a nominally 250-metre grid covering the region of the LiDAR surveys.